Silicon Oxidation and Oxynitridation in the Ultrathin Regime: Ion Scattering Studies

E.P. Gusev, H.C. Lu, T. Gustafsson, and E. Garfunkel

Departments of Chemistry and Physics,
and Laboratory for Surface Modification,
Rutgers University, Piscataway, NJ 08855 - 0939, USA

Received December 15, 1996

The paper reviews our recent studies of the mechanistic and structural aspects of ultrathin (<5 nm) dielectric films (oxides, SiO_2, and oxynitrides, SiO_xN_y) thermally grown on silicon surfaces. High resolution medium energy ion scattering (MEIS) has been used as the primary tool in these studies. We discuss: (i) the growth mechanism of ultrathin films using isotopic ($^{16}O_2/^{18}O_2$) labeling methods, (ii) the initial stages of the interaction of oxygen with silicon surfaces under different temperature and pressure conditions, including a new roughening regime, (iii) the transition region near the oxide/substrate interface, and (iv) silicon oxynitridation in N_2O and NO.

I. Introduction

A simple extrapolation of current scaling trends in ULSI devices indicates that lateral feature sizes below 0.1 μ and gate oxide thicknesses of approximately 4 nm will be required within several years.[1] Furthermore, it now appears that thin silicon oxides and oxynitrides will remain the principle gate dielectric materials in silicon logic and memory devices.[2-5] The electrical properties of these MOS-based devices are strongly correlated with structure and defects at and near the SiO_2/Si interface of the gate oxide, the heart of the MOSFET.[2-4,6-9] However, despite an extensive history of interesting results and stimulating speculation, there are still many open questions concerning dielectric growth and microstructure, especially in the now technologically important ultrathin film regime.[2-4,6-10]

The focus of our studies of ultrathin dielectrics on silicon is to better understand fundamental aspects of the growth and microstructure of ultrathin silicon oxides and oxynitrides on silicon surfaces.[11-17] Below we review our recent progress in understanding the initial oxidation and oxynitridation of silicon by using medium energy ion scattering spectroscopy (MEIS). Following a brief overview of the literature (Section II), we outline the principles of MEIS[18] and discuss sample issues (Section III). Then we discuss the results of the isotopic labeling experiments[11-13,15,17] and their implications concerning the mechanism of oxide film growth (Section IV). Section V is devoted to the interaction of oxygen with silicon at high temperatures in the (sub)monolayer regime and surface roughening.[14] The transition region[15,17] between the crystalline silicon substrate and the amorphous dielectric overlayer film will be discussed in Section VI. Finally (Section VII), we demonstrate the use of MEIS for sub-nm depth profiling of nitrogen in silicon oxynitrides and discuss silicon oxynitridation in N_2O and NO.[16]

II. Silicon oxidation and oxynitridation: background

A number of factors affecting ULSI reliability are known to depend on defects in the silicon-gate oxide interface region, e.g. channel mobility, leakage current, breakdown, and hot-electron induced effects. Although the electrical defects, as detected by C-V, DLTS, EPR, etc. are controlled by the fabrication conditions, there are many open questions concerning the role and atomic configuration of these defects, especially for very thin oxide films.[2-4,6-9,19-21]

Growth Mechanism: The formation of thick oxide

films (>10 nm) is known[4,6,7,22-24] to be described by the Deal-Grove model[25]. According to this model, silicon oxide films grow via molecular diffusion of oxygen to the SiO_2/Si interface and reaction with silicon at the interface. The oxidation kinetics for ultrathin films differ from a simple extrapolation of the Deal-Grove model to thin layers, although this issue is still under debate.[4,6,7,23,24,26-32] Various phenomenological models have been proposed[23] to account for the deviation (in particular, the fast initial growth kinetics), although many require a large number of questionable fitting parameters and do not have direct experimental support. Oxide formation during the initial 0.1-1nm of growth is also not well understood[33-39], and yet it may play a critical role in the formation of gate oxides.

Roughness is one of the factors which is recognized as a critical processing parameter.[40-51] As interface roughness increases, both the breakdown field strength and channel mobility decrease.[40,49,50] However the microscopic origin of interface roughness and the mechanisms causing the interface to roughen are not clear yet. Various surface techniques, including STM and AFM[47,52-55], cross sectional HRTEM[41-43,53], spectroscopic ellipsometry[56,57], optical SHG technique[45], light scattering[51,58], Nomarski microscopy[58], and X-ray diffraction (XRD)[46,59] are used to characterize wafer roughness. Without going into detail, we note that results obtained by these methods frequently differ from each other. A major source of this discrepancy is the different lateral resolution and analyzed areas afforded by each probe.[58] Roughness at a buried interface is even more difficult to characterize than surface roughness.

There is a *transition region* (of altered structure and/or stoichiometry) between crystalline silicon and amorphous SiO_2.[2,7,34,56,60-67] As the thickness of gate dielectrics goes down, the transition region becomes a significant part of the dielectric. The thickness of this region has been reported[2,7,34,56,60-68] to vary from 0.5 nm to 3 nm (even 7 nm [69]), the variations a result of either different oxidation procedures or different measurement techniques, e.g. ellipsometry, photoemission, TEM, etc. Despite extensive work, neither the atomic-scale structure nor the composition (or gradient) in the transition region are well understood - there is currently no universally accepted "conventional" model. Stress[7], microcrystallinity[70], and roughness[42,43,46,53] are all microstructural issues that have been studied with limited success.

Oxynitrides are replacing conventional "pure" silicon gate oxides for sub-0.25 μm devices. Nitrogen incorporated into the oxide has been shown to form a barrier against boron diffusion into and through gate oxides and it also reduces hot-electron degradation.[5,46,71-86] The oxidation of silicon in N_2O is particularly attractive because of O_2 - N_2O processing similarities.[5,72,74,77,78,80,85,87-89] However, among other factors, oxynitridation in N_2O is complicated by the fast gas-phase decomposition of the molecule into N_2, O_2, NO, and O at typical oxidation temperatures (800-1100°C) with the rate and branching ratio of the products strongly dependent on the processing conditions, temperature, residence time, gas flow, and oxidation reactor type (furnace vs. RTP).[77,80,90,91] NO is believed to be responsible for nitrogen incorporation into the film.[75,77,80,82,92] There is still no consensus about what is or should be the optimal nitrogen concentration and distribution. Accurate nitrogen depth profiles have been difficult to measure because of limitations of SIMS[93] and HF etch-back profiling methods. Recent experiments show different nitrogen distributions for RTO vs. furnace grown films[5,80]; NH_3 vs. NO vs. N_2O grown films[5,94]; and following sequential oxidation and oxynitridation processing[84]. Furthermore (directly related to the nitrogen distribution), the growth mechanism of thin oxynitrides, in particular nitrogen incorporation into and concurrent removal from the film, is even less well understood.

III. Experimental

The new results on silicon oxidation and oxynitridation presented in this work were to a large extent due to the use of MEIS[18]. MEIS (Fig. 1) is based on the same principles of ion-solid interactions as is conventional RBS[95,96]. Because of the lower ion energy used in MEIS (97.2 keV protons in our case), and our use of a high resolution torroidal electrostatic ion energy analyzer[97] ($\Delta E/E \sim 0.1\%$), almost monolayer depth resolution can be obtained.[14,98] However, due to the straggling effect[99], the resolution decreases with increasing distance from the surface. Another strength

of MEIS is mass-sensitivity, which enables isotopic labeling experiments[12,13]. The two oxygen isotopes we use (^{18}O and ^{16}O) can be easily distinguished in the film (see Fig. 2).

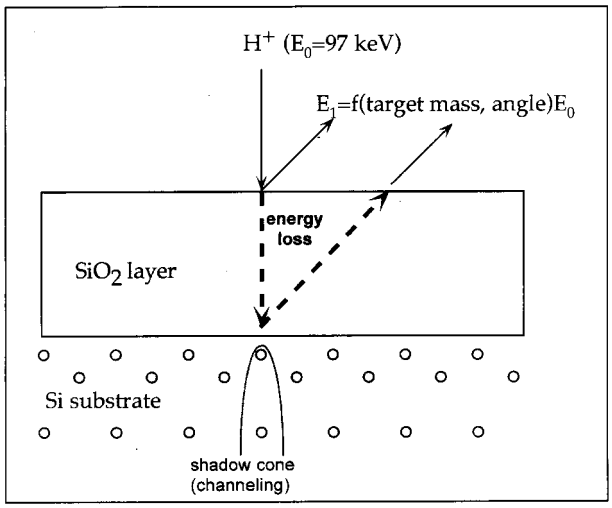

Figure 1. Schematic of medium energy ion scattering.

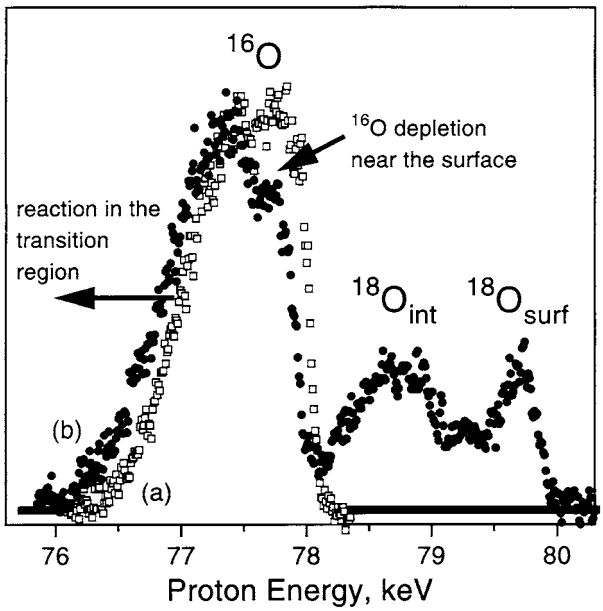

Figure 2. Typical MEIS spectra in the oxygen region before (spectrum a) and after (spectrum b) oxidation of a $Si^{16}O_2$ film in dry $^{18}O_2$ (7 Torr) at 920°C for 1 hour. The energy of the primary proton beam is 97.2 keV; the scattering angle is 125°.

In MEIS, the protons lose energy primarily via electronic excitations while traveling through the solid.[99,100] In the energy spectra, the subsurface species are shifted to lower energies with respect to the surface layer by their energy loss. For the same reason (energy loss), an energy spectrum anticipated for a rough surface differs from one for an ideal smooth surface. In the case of a rough surface, the fraction of protons suffering scattering at the solid/vacuum interface without traveling in the solid (the "effective" surface area) decreases, whereas the fraction of detected protons which traveled through the solid (and their travel length) increases. This results in a lower intensity on the high energy part of the peak and the appearance of a characteristic low-energy tail (see Fig. 4 below). Thus, by examining the peak width and shape, one can learn about the growth mode and surface morphology.[14] Accurate depth distributions of target elements of interest (Si, ^{18}O, ^{16}O, and N) can be deduced from simulations of energy spectra, as discussed in [12]. More details about the MEIS set-up, data acquisition and analysis, and the isotopic labeling technique can be found elsewhere.[11–17]

We examined two set of samples: (i) oxide films grown on Si(100) and Si(111) in UHV chambers, and (ii) ultrathin SiO_2/Si(100) and SiO_xN_y/Si(100) samples grown in industrial (both RTO and furnace) facilities. For the isotopic oxidation experiments (performed in a quartz furnace), both $^{18}O_2/^{16}O_2$ and $^{16}O_2/^{18}O_2$ sequential exposures were used. Isotopic enrichment of $^{18}O_2$ was 95 - 99 %. The moisture level of the oxygen was below 2 ppm. To further reduce any residual water, liquid nitrogen trapping has been used both on the oxygen bottle and adjacent to the furnace during oxidation. Silicon oxynitridation was performed in N_2O or NO ambient at 700 - 1000°C. The final thickness of most films was below 5 nm. Sample preparation conditions are also discussed in the preceding papers.[11–17]

IV. Isotopic labeling experiments

To understand the growth mechanism of ultrathin oxides, we use sequential exposure of Si(100) to oxygen isotopes ($^{16}O_2$ and $^{18}O_2$) in combination with high resolution depth profiling by MEIS.[11–13,15,17] One should mention that isotopic labeling techniques[32,89,101–107] have been used in the past with nuclear reaction analysis (NRA) and secondary ion mass spectroscopy (SIMS) to study oxygen incorporation into relatively thick silicon oxide films. For ultrathin film studies, sub-nm depth resolution is desired, and is only offered by MEIS.

Isotopic labeling MEIS depth profiling allows one not only to look at the oxide thickness but, more important, it provides temporal reaction profiles of incorporated oxygen with near-monolayer depth resolution. Unlike most kinetic studies in the field, this makes it possible to go beyond an examination of the oxide film thickness kinetics and further develop an atomistic picture of oxide formation.

MEIS spectra for a thin $Si^{16}O_2$ film before and after reoxidation in $^{18}O_2$ are shown in Fig. 2. One can see two ^{18}O peaks in the spectra, corresponding to oxygen atoms near the oxide surface (at higher backscattering energies) and to oxygen atoms near the Si/SiO_2 interface. The ^{16}O peak also transforms during reoxidation; the high energy part of the peak is depleted concurrent with the growth of the surface ^{18}O peak. This observation shows that the surface ^{18}O peak is due to (a) surface exchange reaction(s), i.e., as ^{18}O incorporates near the oxide surface, some ^{16}O leaves. One should also note that the ^{16}O peak becomes broader on the low-energy side, implying that the thickness of the ^{16}O-containing oxide layer increases during the reoxidation.

The depth distributions of the isotopes in the film can be obtained by spectral simulations, as explained in Ref.12. A typical example of depth profiles is shown in Fig. 3. The distribution of ^{18}O in this case has two regions with high concentration, one near the outer surface and the other closer to the interface, just as observed in the energy spectrum (Fig. 2). At the same time the amount of ^{16}O near the surface is lower than in the middle of the film such that the total amount of both isotopes in this oxide region remains constant (Fig. 3). This supports the exchange (not growth) hypothesis for the surface reaction. The ^{18}O region near the interface overlaps with the ^{16}O distribution in this region (Fig. 3), inconsistent with the classic Deal-Grove model[25] in which the new $Si^{18}O_2$ oxide should grow right at the interface below the initial $Si^{16}O_2$ layer. Our results show that the reaction occurs throughout the near-interfacial transition region (see below) resulting in the isotopic mixture near the interface. Both the surface exchange reaction and the (near) interface reaction depend on the oxidation conditions. Details of this dependence on pressure, temperature, time and processing conditions, as well as the effect of surface and gaseous impurities (including metals, water, carbon monoxide, and hydrogen) can be found elsewhere.[13,17,108]

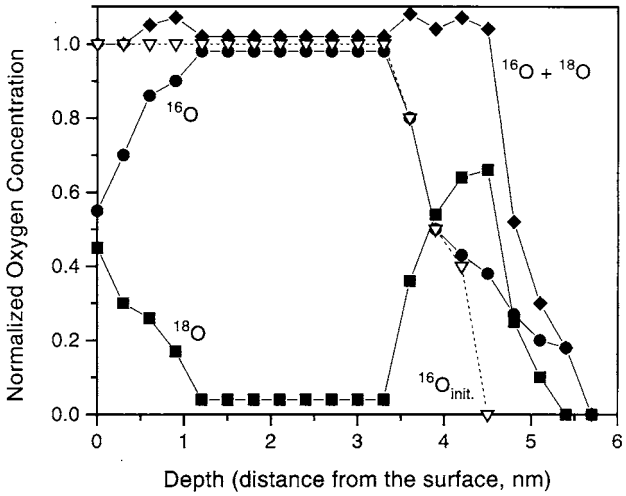

Figure 3. Depth profiles of the oxygen isotopes corresponding to the spectra shown in Fig. 2a (^{16}O - open triangles) and in Fig. 2b (^{16}O - circles, ^{18}O - squares, $^{16}O + ^{18}O$ - diamonds). The oxygen concentration is normalized to the bulk oxide value.

Our results demonstrate that any model of silicon oxidation[25] as a reaction occurring at a well-defined geometrical plane (the SiO_2/Si interface) does not apply to ultrathin films. Isotopic labeling studies here show that the "traditional" interface reaction actually takes place throughout the near-interfacial transition region, and that the surface oxygen exchange reaction is present, and should be considered in any complete model of oxidation. We believe that the near-interfacial reaction is a result of continued oxidation of incompletely oxidized silicon, i.e. suboxides[34,63–65], silicon interstitials[109], silicon monoxide[110] and/or silicon clusters[32,66,67,105]. In this model, the reaction of molecular oxygen with the silicon substrate is not perfect; it occurs with some probability for the generation of the incompletely oxidized silicon atoms which are then consumed by the near-interfacial reaction.[109,111,112] Thin non-stoichiometric region of the oxide near the interface was observed in our work[12,13,15,17,113] and by others[2,7,34,56,60–67]. The surface exchange reaction is less well understood, although observed in earlier studies as well.[32,89,102,103,107,114] Our results show that (for films > 3 nm) the surface exchange reaction occurs independent of the growth reaction near the interface. It has different temperature, pressure, and time dependence and is much more sensitive to external factors, such as, for example, impurities.[17,108] Finally, we note

that the surface reaction may become very important in sub-3 nm oxide films; in this regime the surface and the near-interface reactions overlap in space and, as a result, should affect each other.

V. Initial stages of the interaction of oxygen with Si(111) at low pressures

It is interesting and important to study the very initial stages of the interaction of oxygen with silicon surfaces when the amount of surface oxygen does not exceed one monolayer (1ML = 6.8×10^{14} cm^{-2} for Si(100) and = 7.8×10^{14} cm^{-2} for Si(111)). Low oxygen pressures are required to examine the mechanism of submonolayer oxidation. It is known that very different oxidation modes can occur depending on temperature and oxygen pressure.[33,35,115–124] At low temperatures and high pressures, oxygen interaction with the surface results in oxide growth (Si + O_2 = SiO_2 (s)). In the opposite case (high temperature - low pressure), surface etching via volatile SiO formation occurs (2Si + O_2 = 2 SiO(g)). These oxidation modes are also known as "passive" and "active" oxidation, respectively. Recently, several groups have reported that there is an intermediate ("roughening") regime between the active and passive oxidation modes where the surface morphology qualitatively differs from both pure oxide growth and etching.[54,122,123] In particular, it has been observed by STM[54,122] and HRTEM[123] that the surface becomes very rough if oxidation is performed under these intermediate conditions.

We have used MEIS to study surface morphology and growth (or etching) modes in the passive and active oxidation regimes as well as in the roughening regime.[14] In addition to the high vertical spatial resolution above mentioned, MEIS has several other advantages when compared to "traditional" surface techniques: (i) it provides both structural and compositional information; (ii) the concentration of surface oxygen and displaced silicon atoms can be measured quantitatively; and (iii) local electronic configurations do not affect the data analysis. The three different oxidation modes were probed by tuning the sample temperature on the (p,T) oxidation phase diagram at a constant pressure (10^{-6} Torr in most experiments). MEIS results confirmed the existence of the roughening regime between the active and passive oxidation regime[54,122,123] and most of the discussion below is devoted to this interesting oxidation regime. Our results for the two other (traditional) regimes can be summarized as follows.[14] For passive oxidation, it was shown that bulk (beyond the first monolayer) oxidation does not start before the surface is covered by a surface oxide. We find that the surface oxide is not fully stoichiometric (i.e. SiO_4 unit cell) even at elevated temperatures. Our results in the active oxidation regime are consistent with previous observations[123], i.e. that under conditions when the surface temperature is high and the oxygen flux to the surface is small, volatile SiO forms leaving silicon vacancies on the surface. At high temperatures, the vacancies are mobile and may diffuse far enough to attach to surface steps, resulting in quasi-uniform surface etching via a step flow mechanism[123]. However, under some conditions (near the boundary with the roughening regime), the 2D surface vacancy islands (holes) may nucleate on terraces as a result of a competition between the creation of new vacancies and their diffusion to remote steps. This process and the continuous nucleation of vacancies inside preexisting vacancy islands results in a roughened surface.

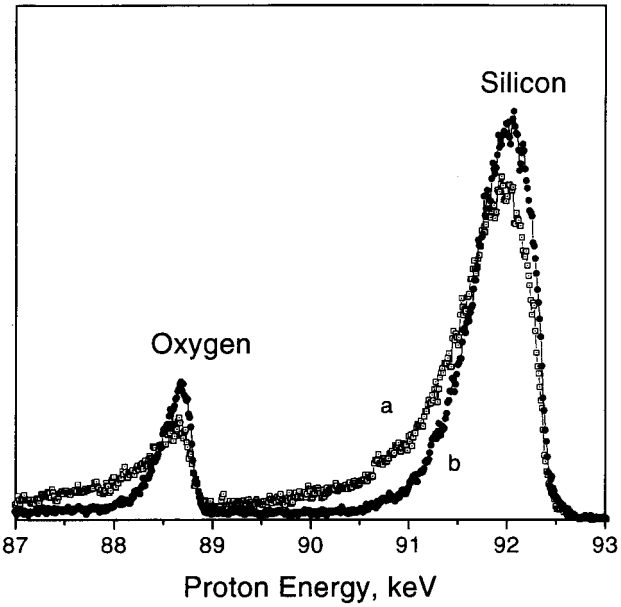

Figure 4. MEIS spectra (both in the oxygen and silicon regions) taken in the roughening regime, in which the Si(111) surface was exposed to oxygen at 770°C and 10^{-6} Torr (spectrum a). For comparison, a spectrum taken in the passive oxidation mode (735°C and 10^{-6} Torr) is also shown (spectrum b). Both spectra show a similar amount of oxygen on the surface, $\sim$ 3 ML. The scattering angle is 74°.

Typical MEIS spectra taken under oxidation conditions corresponding to the roughening regime are shown in Fig. 4. First, both silicon and oxygen peaks are seen in the spectra indicating the presence of oxygen on the

surface. Both peaks show the development of a low-energy tail, which is a fingerprint of surface roughening. By comparing the spectra with those taken under passive and active oxidation conditions, we conclude that we indeed observe a separate region with characteristic roughening behavior. Important questions are: (i) how rough the surface is in the roughening regime, and (ii) what is the limit of MEIS in studying surface roughness. From the known scattering geometry and for the known value of the proton energy loss in silicon of $\sim$ 130 eV/nm[125], one can estimate that the width of the low-energy tail of about 1 keV (Fig. 4) corresponds to $\sim$ 2 - 3 nm "peak-to-peak" roughness with a characteristic lateral scale of less than 10 nm. This roughness is consistent with the value of 4 nm deduced from recent STM experiments on Si(100) at lower oxidation pressures.[126] A separate experiment with 1-2 monolayer holes on the surface shows very little variation of the shape of the energy spectra, which sets the limit of MEIS detection of surface roughness.

Given the fact that the oxygen is present on the surface as oxide islands, surface roughening in this regime can be explained in the following way[54,122,123,126]: it is know that the rate of surface oxide formation on silicon decreases with increasing temperature.[35,37] In the roughening regime, nucleation and growth of the oxide islands becomes very slow. Since the temperature is high enough, surface etching (SiO desorption) occurs between the oxide islands on bare Si at a rate comparable with (or faster than) the lateral oxide growth rate. Etching (SiO desorption) from the oxidized surface areas should be very slow. The surface roughening is thus caused by a competition between continuous surface etching of bare Si regions and surface "passivation" by a surface oxide.

VI. The transition region near the SiO_2/Si interface

For sub-5 nm gate dielectrics, the transition region between the well-ordered Si substrate and the amorphous oxide becomes a significant part of the film. The importance of this region for device performance is determined by the fact that most electrical defects are located near the interface.[2,8,9,21] In addition, our studies suggest that the transition region may be important in understanding the growth reaction near the interface.[12,13,17] There are many publications devoted to experimental and theoretical studies of the SiO_2/Si interface.[2,7,34,56,60–68,127–129] However, the microstructure of the transition region and its role in silicon oxidation and oxynitridation remains unclear. We also note both semantic and conceptual problems of defining the transition region (stress[7,130], roughness[78], suboxides[63,65], density[68,69], composition[12,15], etc.) depending on different probing techniques (ellipsometry, X-ray scattering, photoemission, TEM, MEIS, etc.).

In the oxygen depth profiles deduced from the simulation of the energy spectra of oxygen, we always observe a region near the interface where the oxygen concentration is lower than in the stoichiometric oxide (see Fig. 3). The width of this region is, on average, about 1.2 ± 0.4 nm. At the same time, an analysis of the silicon spectra shows that the silicon concentration is higher than in SiO_2.[12] In a separate experiment, we have studied the ratio between oxygen quantity in the film versus the amount of silicon visible to the proton beam for oxide films of different thickness, from 1.4 to 6 nm.[108] Under channeling conditions, the silicon yield results from scattering of protons by all silicon atoms in the a-SiO_2 film as well as the first subsurface layers of Si substrate. Similar analysis was earlier performed by RBS.[60–62] Our study reveals a perfect SiO_2 stoichiometry for the "bulk" region of the ultrathin films. Most interesting, it shows that there is about 1.4 ML of extra silicon atoms near the interface.

We believe that the width of the transition region observed in our MEIS experiments is due to two main components: roughness and a compositional gradient (suboxide states) (Fig. 5). Strain at the interface may also result in an enhanced probability for the protons to backscatter off substrate atoms located just below the interface. Roughness is know to exist at the Si/SiO_2 interface.[40–51] The RMS value of the interface roughness for high-quality thermal oxides is usually below 0.5 nm, depending on the probing technique and processing conditions. X-ray diffraction experiments performed on oxide films grown in the same reactor and under conditions similar to those of our ultrathin films show about 0.2 - 0.3 nm RMS roughness.[46,59] Surface roughness will also contribute to the MEIS anal-

ysis as our spectra originate from a lateral averaging over a microscopic beam spot. One way to detect a compositional gradient is to monitor suboxide states (Si^{n+}, n=1, 2, 3) by core-level (Si2p) photoemission of the SiO_2/Si system.[32,34,36,63–65,131–135] Our recent synchrotron-based photoemission studies[113] of ultrathin (1 - 3 nm) oxide films on Si(100) (also analyzed by MEIS) show suboxide states near the interface corresponding to $\sim$ 1.5 ML, consistent with some of the earlier studies[63,135]. According to recent *ab-initio* calculations[127,128], this value of the suboxide states corresponds to, at least, 0.5 nm of non-stoichiometric oxide near the interface. The near-interfacial suboxides, even though they may have a low steady-state concentration ($\sim$ 1 ML) are quite important. They should have a higher reactivity towards inward diffusing oxygen than the substrate silicon, and could explain the breadth of the transition region. Finally, we note that a better cross-correlation of different techniques on the same samples is needed to further understand the complexity of the SiO_2/Si interface at atomic level.

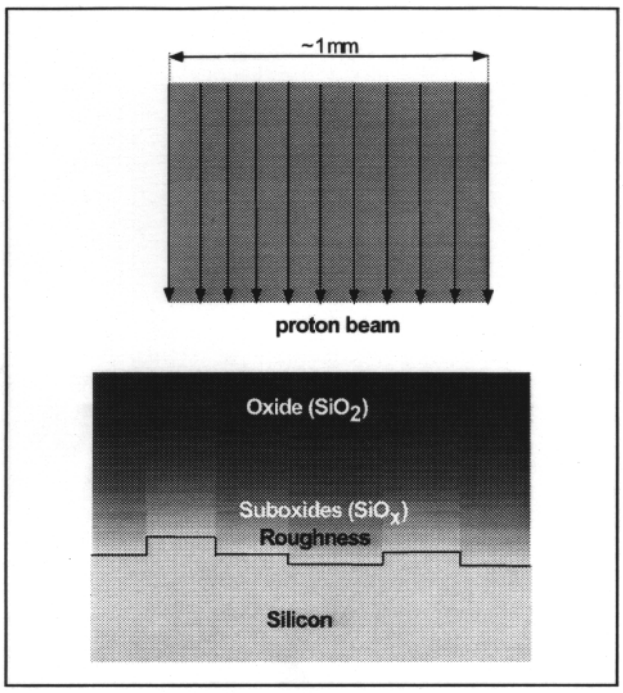

Figure 5. A model demonstrating how MEIS is used to study the transition region near the $Si0_2$/Si interface.

VII. Ultrathin oxynitride films

As the thickness of the gate oxide in microelectronic devices decreases, several new technological and scientific issues must be solved to maintain high reliability levels. Hot electron induced degradation, boron penetration through ultrathin oxides, and electrical defects at the interface are among the most important factors that determine device performance. It has recently been demonstrated that oxynitride (SiO_xN_y) gate dielectrics have a number of properties superior to conventional pure SiO_2 oxides. The use of oxynitrides suppresses boron penetration, improves hot-electron immunity and decreases interface defects.[5,71,72,74–78,82,83,86] However, despite an increasing number of studies of ultrathin oxynitrides using various techniques (XPS, NRA, SIMS, ellipsometry, EPR and electrical characterization methods) [5,71,72,74–78,82,83,86,89,92,94,136], several fundamental questions, in particular the oxynitridation mechanism, and the mechanism(s) behind the beneficial role of nitrogen, are still not well understood.

It is clear now that the distribution of nitrogen in the film is an important factor governing the improved properties of oxynitrides. Unfortunately, determining an accurate distribution of the nitrogen in ultrathin films is an analytical challenge; most depth profiling techniques (such as SIMS, HF etchback techniques and Ar^+ sputtering methods) do not usually provide the required sub-nm depth resolution. We have used the high depth resolution and mass sensitivity of MEIS to analyze ultrathin oxynitrides.[16,137,138] In particular, we have studied the growth mechanism and composition of ultrathin oxynitrides thermally grown on Si(100) in N_2O, NO, and sequential oxidation-nitridation. Both furnace and rapid thermal oxidation (in the temperature range of 700 - 1000°C) have been explored.

Accurate profiles of nitrogen in the films were analyzed.[16] We showed that, for a thin SiO_2 pre-oxide annealed in NO, the nitrogen atoms incorporate within $\sim$ 1.5 nm of the SiO_xN_y/Si interface. Oxynitridation of clean Si(100) in NO results in very thin films ($\sim$ 1.5 - 2.5 nm after 1 hour oxidation at atmospheric pressure) with a more uniform nitrogen distribution (Fig. 6). The widths of the nitrogen distribution, the total amount of N in the film, and the ratio of nitrogen to oxygen increase with increasing temperature. We did not see a significant amount of nitrogen on the substrate side of the interface (Fig. 6). Oxynitridation in N_2O results in a lower concentration of nitrogen incorporated into the film (Fig. 6), consistent with other

studies[83]. We observed a broader distribution of nitrogen in the film in the case of furnace N_2O oxynitridation, as compared to rapid thermal oxynitridation in N_2O, in agreement with earlier observations[80].

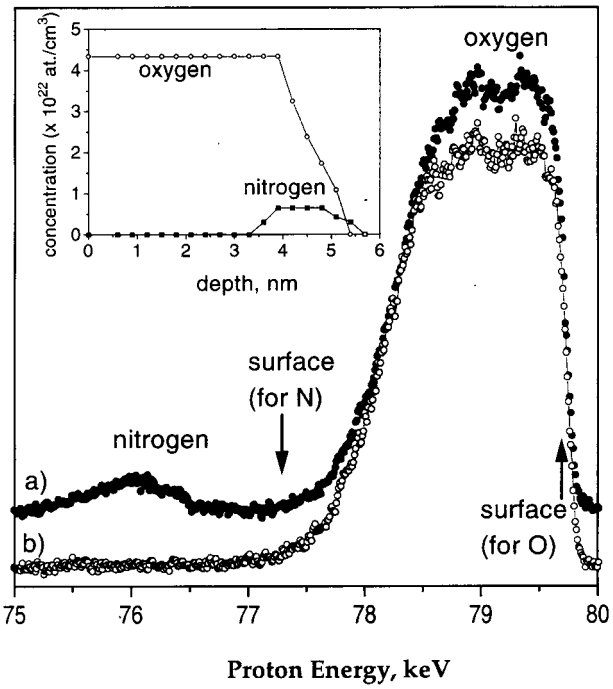

Figure 6. An example demonstrating the use of MEIS for silicon oxynitridation studies. Spectrum a) corresponds to $\sim$ 5 nm oxynitride film grown in a furnace in O_2 (850°C, 5.5 min) followed by NO (950°C, 60 min.). This spectrum shows about 1.1×10^{15} N/cm^{-2}. Oxynitride film of similar thickness grown in N_20 at 850°C for 110 min. (spectrum b) shows much less nitrogen (and broader distribution). The oxygen and nitrogen depth profiles corresponding to the spectrum a) are shown in the inset.

It has recently been shown that nitrogen removal from the film occurs during silicon oxynitridation in N_2O.[80,84] There are at least two hypotheses on the mechanism of N removal: Carr et. al[80] propose that atomic oxygen causes nitrogen removal, whereas Saks et.al[84] argue that NO is responsible for N removal from the film. To further elucidate the role of NO in nitrogen incorporation and nitrogen removal, we have performed sequential exposures of Si (at 850°C, furnace) to NO, O_2, and then NO (NO/O_2/NO) and analyzed the resultant depth profiles. This experiment clearly shows that NO does not efficiently remove N from the oxynitride. Atomic oxygen remains a possible candidate to be responsible for N removal, although further studies are required to clarify the role of atomic oxygen. Exposure to ozone (an effective atomic oxygen source) also results in nitrogen removal, supporting the atomic oxygen model.[80]

The presence of nitrogen in oxynitrided films is known to retard the oxidation kinetics.[139,140] To understand the mechanism of this retardation, oxynitride films with different amounts of nitrogen near the SiO_xN_y/Si interface and pure ("control") SiO_2/Si films were reoxidized in dry $^{18}O_2$ under equivalent conditions[137] and the spatial distribution of the ^{18}O incorporated into the films was analyzed by high-resolution depth profiling methods[12,13]. Analogous to the pure SiO_2 case[12,13,89], we observed two distinct regions where oxygen incorporation into the oxynitride films occurs during high-temperature oxidation: at/near the interface and near the outer oxide surface.[137] The (near)interface growth reaction is found to be significantly retarded in the presence of the interfacial nitrogen (with a higher degree of the retardation for higher concentrations of nitrogen). The presence of nitrogen near the interface does not effect the surface exchange reaction.

Summary

As the gate dielectrics thickness in ULSI devices shrinks below 5 nm, an atomic scale understanding of the physical and chemical processes occurring in such ultrathin films becomes more critical. In this work, we have used high resolution medium energy ion scattering, a technique which provides sub-nm depth resolution, to study ultrathin silicon oxides and oxynitrides. Several new and interesting features of the growth and composition of these dielectrics have been observed. By using isotopic ($^{18}O_2/^{16}O_2$) labeling methods we directly observe oxidation reactions in two spatially distinct regions: an oxide growth reaction throughout the near-SiO_2/Si interface region, and an exchange reaction of the oxygen isotopes near the outer oxide surface. This behavior is inconsistent with the traditional (Deal-Grove) model of silicon oxidation. Our results also support the existence of a thin ($\sim$ 1 nm) transition region between the silicon substrate and the amorphous stoichiometric oxide overlayer, although the detailed microstructure of this region is still unclear. For oxidation at low oxygen pressures, in addition to observing oxide growth and surface etching (occurring at

low and high temperatures respectively), surface roughening results for intermediate temperature oxidation. Finally, we have demonstrated the use of MEIS for silicon oxynitridation studies by accurately determining the nitrogen depth distribution.

Acknowledgments

The authors would like to thank M. Green, L. Feldman, D. Buchanan, E. Poindexter, I. Baumvol, J.J. Ganem, I. Trimaille, T. Madey and H.S. Tao who were involved in different aspects of this work and in discussions. Partial support for this work has come from National Science Foundation (DMR-9408578 and ECS-9530984), ACS-PRF (28788-AC5), and the NJ-AIMS program.

References

1. Y. Taur, Y. J. Mii, D. J. Frank, H. S. Wong, D. A. Buchanan, S. J. Wind, S. A. Rishton, G. A. Sai-Halasz, and E. J. Nowak, IBM Res. Develop. **39**, 245 (1995).
2. C. R. Helms and E. H. Poindexter, Rep. Prog. Phys. **57**, 791 (1994).
3. G. Kamarinos and P. Felix, J. Phys. D **29**, 487 (1996).
4. C. J. Sofield and A. M. Stoneham, Semic. Sci. Technol. **10**, 215 (1995).
5. M. L. Green, in *Advances in Rapid Thermal and Integrated Processing,* edited by F. Roozeboom (Plenum Press, New York - London, 1995), p. 193.
6. *The Si-SiO_2 System*, edited by P. Balk (Elsevier, Amsterdam, 1988).
7. E. Irene, Crit. Rev. Sol. St. Mat. Sci. **14**, 175 (1988).
8. E. H. Poindexter and W. L. Warren, J. Electrochem. Soc. **142**, 2508 (1995).
9. E. H. Poindexter, Semic. Sci. Technol. **4**, 961 (1989).
10. F. H. P. M. Habraken and A. E. T. Kuiper, Materials Sci. and Eng. Rept. **R12**, 123 (1994).
11. E. P. Gusev, H. C. Lu, T. Gustafsson and E. Garfunkel, in *Interface Control of Electrical, Chemical, and Mechanical Properties,* edited by S. P. Murarka, K. Rose, T. Ohmi, and T. Seidel (MRS, 1994), p. 69.
12. E. P. Gusev, H. C. Lu, T. Gustafsson and E. Garfunkel, Phys. Rev. B**52**, 1759 (1995).
13. H. C. Lu, T. Gustafsson, E. P. Gusev and E. Garfunkel, Appl. Phys. Lett. **67**, 1742 (1995).
14. H. C. Lu, E. P. Gusev, E. Garfunkel and T. Gustafsson, Surf. Sci. **341**, 111 (1996).
15. E. P. Gusev, H. C. Lu, T. Gustafsson and E. Garfunkel, Appl. Surf. Sci. **104/105**, 329 (1996).
16. H. C. Lu, E. P. Gusev, T. Gustafsson, E. Garfunkel, M. L. Green, D. Brasen and L. C. Feldman, Appl. Phys. Lett. **69**, 2713 (1996).
17. E. P. Gusev, H. C. Lu, T. Gustafsson and E. Garfunkel, in *The Physics and Chemistry of SiO_2 and the Si-SiO_2 Interface - 3.* edited by H. Z. Massoud, E. H. Poindexter, and C. R. Helms (The Electrochemical Soc., Pennington, NJ, 1996),p.49.
18. J. F. van der Veen, Surf. Sci. Rept. **5,** 199 (1985).
19. E. Cartier and D. J. DiMaria, Microelectronic Engineering **22**, 207 (1993).
20. J. H. Stathis, D. A. Buchanan, D. L. Quinlan, A. H. Parsons and D. E. Kotecki, Appl. Phys. Lett. **62**, 2682 (1993).
21. J. F. Conley and P. M. Lenahan, in *The Physics and Chemistry of SiO_2 and the Si-SiO_2 Interface - 3.* edited by H. Z. Massoud, E. H. Poindexter and C. R. Helms (The Electrochemical Soc., Pennington, NJ, 1996), p. 214.
22. J. Blank, in *The Physics and Chemistry of SiO_2 and the Si-SiO_2 Interface*, edited by C. R. Helms and B. E. Deal (Plenum Press, NY, 1988), p. 1.
23. B. E. Deal, in *The Physics and Chemistry of SiO_2 and the Si-SiO_2 Interface,* edited by C. R. Helms and B. E. Deal (Plenum Press, NY, 1988), p. 5.
24. A. Atkinson, Rev. Mod. Phys. **57**, 437 (1985).
25. B. E. Deal and A. S. Grove, J. Appl. Phys. **36**, 3770 (1965).
26. S. C. Kao and R. H. Doremus, in *The Physics and Chemistry of SiO_2 and the Si-SiO_2 Interface - 2*, edited by C. R. Helms and B. E. Deal (Plenum Press, N.Y., 1993), p. 23.
27. R. H. Doremus and S. C. Kao, in *Interface Control of Electrical, Chemical, and Mechanical Properties.* edited by S. P. Murarka, K. Rose, T. Ohmi, and T. Seidel (MRS, 1994), p. 53.
28. H. Z. Massoud, J. D. Plummer and E. A. Irene, J. Electrochem. Soc. **132**, 2693 (1985).
29. H. Z. Massoud, J. D. Plummer and E. A. Irene, J. Electrochem. Soc. **132**, 1745 (1985).
30. N. F. Mott, S. Rigo, F. Rochet and A. M. Stoneham, Phil. Mag. B.**60**, 189 (1989).

31. A. M. Stoneham, C. R. M. Grovenor and A. Cerezo, Phil. Mag. B**55**, 201 (1987).
32. F. Rochet, S. Rigo, M. Froment, C. d'Anterroches, C. Maillot, H. Roulet and G. Dufour, Adv. Phys. **35**, 339 (1986).
33. T. Engel, Surf. Sci. Rep. **18**, 91 (1993).
34. T. Hattori, CRC Crit. Rev. Solid State Mater. Sci. **20**, 339 (1995).
35. V. D. Borman, E. P. Gusev, Y. Y. Lebedinski and V. I. Troyan, Phys. Rev. B**49**, 5415 (1994).
36. V. D. Borman, E. P. Gusev, Y. Y. Lebedinski and V. I. Troyan, Phys. Rev. Lett. **67**, 2387 (1991).
37. M. Tabe, T. T. Chiang, I. Lindau and W. E. Spicer, Phys. Rev. B**34**, 2706 (1986).
38. Y. Ono, M. Tabe and H. Kageshima, Phys. Rev. B **48**, 14291 (1993).
39. P. Avouris and D. Cahill, Ultramicroscopy **42/44**, 838 (1992).
40. P. O. Hahn and M. Henzler, J. Vac. Sci. Tech. **A2**, 574 (1984).
41. S. M. Goodnick, D. K. Ferry, C. M. Wilmsen, Z. Liliental, D. Fathy, and O. L. Krivanek, Phys. Rev. B **32**, 8171 (1985).
42. H. Akutsu, Y. Sami and I. Ohdomari, Phys. Rev. B **44**, 1616 (1991).
43. A. H. Carim and A. Bhattacharyya, Appl. Phys. Lett.**46**, 872 (1985).
44. A. H. Carim and R. Sinclair, J. Electrochem. Soc. **134**, 741 (1987).
45. J. I. Dadap, B. Doris, Q. Deng, M. C. Downer, J. K. Lowell and A. C. Diebold, Appl. Phys. Lett. **64**, 2139 (1994).
46. M. L. Green, D. Brasen, K. W. Evans-Lutterodt, L. C. Feldman, K. Krisch, W. Lennard, H. T. Tang, L. Manchanda and M. T. Tang, Appl. Phys. Lett. **65**, 848 (1994).
47. M. Hirose, M. Hiroshima, T. Yasaka, M. Takakura and S. Miyazaki, Microelectronic Engineering **22**, 3 (1993).
48. M. Niwa, T. Kouzaki, K. Okada, M. Udagawa and R. Sinclair, Jpn. J. Appl. Phys. **33,** 388 (1994).
49. T. Ohmi, K. Kotani, A. Teramoto and M. Miyashita, IEEE Electron. Device Lett. **12**, 652 (1991).
50. T. Ohmi, M. Miyashita, M. Itano, T. Imaoka and I. Kawanabe, IEEE Trans. Electr. Dev. **39**, 537 (1992).
51. A. Ross, M. Bergkvist and C. G. Ribbing, Appl. Optics **27**, 4660 (1988).
52. M. Niwa, H. Iwasaki, Y. Watanabe, I. Sumita, N. Akutsu and Y.Akutsu, Appl. Surf. Sci. **60/61**, 39 (1992).
53. M. Niwa, M. Udagawa, K. Okada, T. Kouzazki and R. Sinclair, Appl. Phys. Lett. **63**, 675 (1993).
54. J. Seiple and J. P. Pelz, J. Vac. Sci. Tech. A **13**, 772 (1995).
55. M. Suzuki, Y. Homma, Y. Kudoh and N. Yabumoto, Jpn. J. Appl. Phys. **32**, 1419 (1993).
56. V. A. Yakovlev, Q. Liu and E. Irene, J. Vac. Sci. Technol. B**10**, 427 (1992).
57. N. V. Nguyen, D. Chandler-Horowitz, P. M. Amirtharaj and J. G. Pellegrino, Appl. Phys. Lett. **64**, 2688 (1994).
58. I. J. Malik, S. Pirooz, L. W. Shive, A. J. Davenport and C. M. Vitus, J. Electrochem. Soc. **140**, L75 (1993).
59. M. T. Tang, K. W. Evans-Lutterodt, G. S. Higashi and T. Boone, Appl. Phys. Lett **62**, 3144 (1993).
60. N. W. Cheung, L. C. Feldman, P. J. Silverman and I. Stensgaard, Appl. Phys. Lett. **35**, 859 (1979).
61. R. Haight and L. C. Feldman, J. Appl. Phys. **53**, 4884 (1982).
62. L. C. Feldman, in *The Physics and Chemistry of SiO_2 and the Si-SiO_2 Interface,* edited by C. R. Helms and B. E. Deal (Plenum Press, NY, 1988), p. 199.
63. F. J. Himpsel, F. R. McFeely, A. Taleb-Ibrahimi, J. A. Yarmoff and G. Hollinger, Phys. Rev. B **38**, 6084 (1988).
64. P. J. Grunthaner, M. H. Hecht, F. J. Grunthaner and N. M. Johnson, J. Appl. Phys. **61**, 629 (1987).
65. F. J. Grunthaner and P. J. Grunthaner, Mat. Sci. Rep. **1**, 65 (1986).
66. P. E. Batson, Nature **366**, 727 (1993).
67. P. E. Batson, N. D. Browning and D. A. Muller, Microsc. Soc. Amer. Bulletin **24**, 371 (1994).
68. N. Awaji, Y. Sugita, T. Nakanishi, S. Ohkubo, K. Takasaki and S. Komiya, J. Vac. Sci. Technol. A **14**, 971 (1996).
69. E. Hasegawa, A. Ishitani, K. Akimoto, M. Tsukiji and N. Ohta, J. Electrochem. Soc. **142**, 273 (1995).
70. A. Ourmazd, D. W. Taylor, J. A. Rentscheir and J. Bevk, Phys. Rev. Lett. **53**, 743 (1987).
71. H. Hwang, W. Ting, B. Maiti, D. L. Kwong and J. Lee, Appl. Phys. Lett. **57**, 1010 (1990).
72. H. Fukuda, T. Arakawa and S. Ohno, Jpn. J.

Appl. Phys. **29**, L2333 (1990).
73. W. Ting, H. Hwang, J. Lee and D. L. Kwong, J. Appl. Phys. **70**, 1072 (1991).
74. E. C. Carr and R. A. Buhrman, Appl. Phys. Lett. **63**, 54 (1993).
75. S. Dimitrijev, D. Sweatman and H. B. Harrison, Appl. Phys. Lett. **62**, 1539 (1993).
76. M. Bhat, G. W. Yoon, J. Kim and D. L. Kwong, Appl. Phys. Lett. **64**, 2116 (1994).
77. P. J. Tobin, Y. Okada, S. A. Ajuria, V. Lakhotia, W. A. Feil and R. I. Hedge, J. Appl. Phys. **75**, 1811 (1994).
78. M. L. Green, D. Brasen, K. W. Evans-Lutterodt, L. C. Feldman, K. Krisch, W. Lennard, H. T. Tang, L. Manchanda and M. T. Tang, Appl. Phys. Lett. **65**, 848 (1994).
79. S. V. Hattangady, H. Niimi and G. Lucovsky, Appl. Phys. Lett. **66**, 3495 (1995).
80. E. C. Carr, K. A. Ellis and R. A. Buhrman, Appl. Phys. Lett. **66**, 1492 (1995).
81. D. Landheer, Y. Tao, D. X. Xu, G. I. Sproule and D. A. Buchanan, J. Appl. Phys. **78**, 1818 (1995).
82. R. I. Hedge, P. J. Tobin, K. G. Reid, B. Maiti and S. A. Ajuria, Appl. Phys. Lett. **66**, 2882 (1995).
83. M. Bhat, L. K. Han, D. Wristers, J. Yan, D. L. Kwong and J. Fulford, Appl. Phys. Lett. **66**, 1225 (1995).
84. N. S. Saks, D. I. Ma and W. B. Fowler, Appl. Phys. Lett. **67**, 374 (1995).
85. D. M. Fleetwood and N. M. Saks, J. Appl. Phys. **79**, 1583 (1996).
86. D. Wristers, L. K. Han, T. Chen, H. H. Wang and D. L. Kwong, Appl. Phys. Lett. **68**, 2094 (1996).
87. K. A. Ellis and R. A. Buhrman, Appl. Phys. Lett. **68**, 1696 (1996).
88. Z. H. Lu, S. P. Tay, R. Cao and P. Pianetta, Appl. Phys. Lett. **67**, 2836 (1995).
89. J. J. Ganem, S. Rigo, I. Trimaille, I. J. R. Baumvol and F. C. Stedile, Appl. Phys. Lett. **68**, 2366 (1996).
90. M. Hartig and P. J. Tobin, J. Electrochem. Soc. **143**, 1753 (1996).
91. A. Gupta, Y. Li, E. Gusev and E. Garfunkel, to be published.
92. I. J. R. Baumvol, F. C. Stedile, J. J. Ganem, I. Trimaille and S. Rigo, Appl. Phys. Lett. **69**, 2385 (1996).
93. M. R. Frost and C. W. Magee, Appl. Surf. Sci. **104/105**, 379 (1996).
94. I. J. R. Baumvol, F. C. Stedile, J. J. Ganem, I. Trimaille and S. Rigo, J. Electrochem. Soc. **143**, 2938 (1996).
95. L. C. Feldman, J. W. Mayer and S. T. Picraux, *Materials Analysis by Ion Channeling* (Academic Press, NY, 1982).
96. L. C. Feldman, Surf. Sci. **299/300**, 233 (1994).
97. R. M. Tromp, M. Copel, M. C. Reuter, M. H. van Hoegen, J. Speidell and R. Koudijs, Rev. Sci. Instrum. **62**, 2679 (1991).
98. J. Vrijmoeth, P. M. Zagwijn, J. W. M. Frenken and J. F. van der Veen, Phys. Rev. Lett. **67**, 1134 (1991).
99. F. Besenbacher, J. U. Andersen, and E. Bonderup, Nucl. Instr. Meth. **168**, 1 (1980).
100. P. F. A. Alkemade, W. C. Turkenburg and W. F. van der Weg, Nucl. Instr. Meth. B **28**, 161 (1987).
101. E. Rosencher, A. Straboni, S. Rigo and G. Amsel, Appl. Phys. Lett. **34**, 254 (1979).
102. F. Rochet, B. Agius and S. Rigo, J. Electrochem. Soc. **131**, 914 (1984).
103. C. J. Han and C. R. Helms, J. Electrochem. Soc. **135**, 1824 (1988).
104. R. J. Hussey, D. A. Bisaillion, G. I. Sproule and M. J. Graham, Corros. Sci. **35**, 917 (1993).
105. J. J. Ganem, G. Battistig, S. Rigo and I. Trimaille, Appl. Surf. Sci. **65/66**, 647 (1993).
106. M. P. Murrell, C. J. Sofield and S. Sugden, Phil. Mag. B **63**, 1277 (1991).
107. F. C. Stedile, I. J. R. Baumvol, J. J. Ganem, S. Rigo, I. Trimaille, G. Battistig, W. H. Schulte and H. W. Becker, Nucl. Instr. Meth. B **85**, 248 (1994).
108. H. C. Lu, Ph.D. Thesis, Rutgers University, 1997.
109. W. A. Tiller, J. Electrochem. Soc. **128**, 689 (1981).
110. S. I. Raider, in *The Physics and Chemistry of SiO_2 and the Si-SiO_2 Interface,* edited by C. R. Helms and D. E. Deal (Plenum Press, NY, 1988), p. 35.
111. S. T. Dunham, in *The Physics and Chemistry of SiO_2 and the Si-SiO_2 Interface,* edited by C. R. Helms and B. E. Deal (Plenum Press, NY, 1988), p. 477.
112. S. T. Dunham and J. D. Plummer, J. Appl. Phys. **59**, 2541 (1986).
113. H.-S. Tao, E. P. Gusev, H. C. Lu, T. E. Madey, T. Gustafsson, E. Garfunkel and J. Rowe, to be published.

114. I. Trimaille and S. Rigo, Appl. Surf. Sci. **39**, 65 (1989).
115. J. J. Lander and J. Morrison, J. Appl. Phys. **33**, 2089 (1962).
116. F. W. Smith and G. Ghidini, J. Electrochem. Soc. **129**, 1300 (1982).
117. M. P. D'Evelyn, M. M. Nelson and T. Engel, Surf. Sci. **186**, 75 (1987).
118. M. R. Baklanov, V. N. Kruchinin, S. M. Repinsky and A. A. Shklyaev, React. Solids **7**, 1 (1989).
119. A. A. Shklyaev and T. Suzuki, Phys. Rev. Lett. **75**, 272 (1995).
120. J. R. Engstrom, D. J. Bonser and T. Engel, Surf. Sci. **268**, 238 (1992).
121. A. Feltz, U. Memmert and R. J. Behm, Chem. Phys. Lett. **192**, 271 (1992).
122. A. Feltz, U. Memmert and R. J. Behm, Surf. Sci. **314**, 34 (1994).
123. F. M. Ross, J. M. Gibson and R. D. Twesten, Surf. Sci. **310**, 243 (1994).
124. J. Seiple, J. Pecquet, Z. Meng and J. P. Pelz, J. Vac. Sci. Tech. A **11**, 1649 (1993).
125. H. H. Andersen and J. F. Ziegler, *Hydrogen Stopping Powers and Ranges in All Elements*, Vol. 3 (Pergamon Press, New York, 1977).
126. J. Seiple and J. P. Pelz, Phys. Rev. Lett. **73**, 999 (1994).
127. A. Pasquarello, M. S. Hybertsen and R. Car, Phys. Rev. B **53**, 10942 (1996).
128. A. Pasquarello, M. S. Hybertsen and R. Car, Phys. Rev. Lett. **74,** 1024 (1995).
129. H. Kageshima and M. Tabe, in *Control of Semiconductor Interfaces*, edited by I. Ohdomari, M. Oshima, and A. Hiraki (Elsevier, Amsterdam, 1994), p. 227.
130. C. H. Bjorkman, J. T. Fitch and G. Lucovsky, Appl. Phys. Lett. **56**, 1983 (1990).
131. F. J. Himpsel, D. A. Lapiano-Smith, J. F. Morar and J. Bevk, in *The Physics and Chemistry of SiO_2 and the Si-SiO_2 Interface*, II, edited by C. R. Helms and B. E. Deal (Plenum Press, NY, 1993), p. 237.
132. F. J. Grunthaner, P. J. Grunthaner, R. P. Vasquez, B. F. Lewis, J. Maserjian and A. Madhukar, Phys. Rev. Lett. **43**, 1683 (1979).
133. M. M. Banaszak-Holl and F. R. McFeely, Phys. Rev. Lett. **71**, 2441 (1993).
134. F. R. McFeely, K. Z. Zhang, M. M. Banaszak-Hall, S. Lee and J. E. Bender-IV, J. Vac. Sci. Technol. B **14**, 2824 (1996).
135. Z. H. Lu, M. J. Graham, D. T. Jiang and K. H. Tan, Appl. Phys. Lett. **63**, 2941 (1993).
136. E. A. Irene, Q. Liu, W. M. Paulson, P. J. Tobin and R. I. Hedge, J. Vac. Sci. Technol. B **14**, 1697 (1996).
137. H. C. Lu, E. P. Gusev, E. Garfunkel and T. Gustafsson, J. Appl. Phys., in press.
138. E. P. Gusev, H. C. Lu, T. Gustafsson, E. Garfunkel, M. L. Green and D. Brasen, Appl. Phys. Lett., in press.
139. S. I. Raider, R. A. Gdula and J. R. Petrak, Appl. Phys. Lett. **27**, 150 (1975).
140. M. L. Green, D. Brasen, L. C. Feldman, W. Lennard and H. T. Tang, Appl. Phys. Lett. **67**, 1600 (1995).